

**PLURONIC F-127 COATED ZINC OXIDE
NANOPARTICLES CYTOTOXICITY AND THEIR
PHOTODYNAMIC THERAPY TOWARDS
HUMAN RT4 URINARY BLADDER CANCER
CELL LINES**

ABDUSALAM ALI SOUD ABUELSAMEN

UNIVERSITI SAINS MALAYSIA

2019

**PLURONIC F-127 COATED ZINC OXIDE
NANOPARTICLES CYTOTOXICITY AND THEIR
PHOTODYNAMIC THERAPY TOWARDS
HUMAN RT4 URINARY BLADDER CANCER
CELL LINES**

by

ABDULSALAM ALI SOUD ABUELSAMEN

**Thesis submitted in fulfilment of the requirements
for the degree of
Doctor of Philosophy**

November 2019

DEDICATION

I dedicate this work to our first teacher, Prophet Mohammed Bin Abdullah (Peace be upon him) who is the envoy of mercy to the humanity, and who leads us out of the darkness of disbelief and polytheism to the light of belief in the oneness of Allah Almighty. I also dedicate this thesis to my mother, my father, my wife and my family. May Allah make this work in the balance of their good deeds.

With my respect

ACKNOWLEDGEMENT

In the Name of Allah, the Most Beneficent, the Most Merciful.

All praise and thanks are due to the **Almighty ALLAH SUBHANH WA TAALA**, the Lord of the world, for giving me the health, strength, knowledge and patience to complete this thesis, words are not enough to bestow thanks and praise to the **Almighty ALLAH**.

I would like to express my deep gratitude to my main supervisor Associate Professor Dr. Shahrom Mahmud for all his support, patience and guidance during this research. His contribution as a teacher has widened my horizon in conducting the research especially through his wisdom and relentless encouragement. Furthermore, my appreciation and sincere gratitude go to my co-supervisors Associate Professor Dr. Amin Malik Shah Abdul Majid for providing valuable scientific input, constructive criticism, support and encouragement. I am deeply indebted to Dr. Noor Haida Mohamed Khaus, for her technical input and help in the preparation of polymer-based surface modified ZnO NPs at her research laboratory in School of Chemistry, USM. I am privileged to be under the supervision of these supervisors during the Ph.D research years. As well as, I would like to express my gratitude to my friend Dr. Fouad Saleih R. Al-Suede, who is not only a friend but a brother, for all his help and guidance in cancer tests at toxicology laboratories in EMAN Biodiscoveries Sdn Bhd.

I would like to thank Universiti Sains Malaysia and EMAN Biodiscoveries Sdn Bhd for giving me the opportunity and providing me with all the necessary facilities that made my study possible. Moreover, I would like to express my gratitude and thanks to all School of Physics faculty members, technicians, and administrative staff. My acknowledgement also goes to laboratory members of NOR Lab for their help in getting the characterisation of ZnO properties, and to the electron microscopy unit at

School of Biology, USM for their technical help. I also like to acknowledge all my colleagues and ZORI members for their cooperation and those whose names I may have missed to mention here for all their support and help during my PhD study.

Last but not the least, I would like to express my sincere gratitude to my beloved family who are always in my heart; my beloved mother, father, wife, my wonderful children Anas and Sarra, my dearest brothers and sisters for all their continuous prayers, support, love, inspiration and encouragement which without I would have not been able to complete my studies.

*Abdulsalam Ali Soud Abuelsamen,
Penang, Malaysia, November 2019.*

TABLE OF CONTENTS

ACKNOWLEDGEMENT	ii
TABLE OF CONTENTS	iv
LIST OF TABLES	viii
LIST OF FIGURES	ix
LIST OF SYMBOLS	xiii
LIST OF ABBREVIATIONS	xv
ABSTRAK	xvii
ABSTRACT	xix
CHAPTER 1 INTRODUCTION	1
1.1 Nanotechnology	1
1.2 Zinc Oxide	1
1.3 Cancer	2
1.4 Photodynamic therapy	2
1.5 Motivation and Problem statement	3
1.6 Objectives	4
1.7 Scope of the study	4
1.8 Thesis Originality	5
1.9 Thesis outline	5
CHAPTER 2 LITERATURE REVIEW	7
2.1 Introduction	7
2.2 Zinc Oxide	7
2.3 ZnO crystal structure	8
2.4 Optical properties	10
2.5 Toxicity of ZnO: Mechanism and main key factors	13
2.5.1 The intercellular release of (Zn ²⁺) from the ZnO NPs	14
2.5.2 The generation of reactive oxygen species (ROS)	15

2.5.3	Main toxicity key factors	18
2.6	Pluronic F127 surfactant	20
2.6.1	Pluronic F-127 as a surfactant for NPs in biomedical application	22
2.6.2	Pluronic F-127 coated ZnO nanoparticles	24
2.7	Bladder Cancer	24
2.8	Conventional treatment for Bladder cancer	26
2.9	The anticancer activity of ZnO NPs	27
2.10	Photodynamic therapy	31
2.10.1	History of PDT	32
2.10.2	Photodynamic Reactions	33
2.10.3	Photosensitizers	34
2.11	ZnO nanoparticles for photodynamic therapy	36
2.12	Cell death morphological patterns.	45
CHAPTER 3 EXPERIMENTAL PROCEDURE		48
3.1	Introduction	48
3.2	Synthesis of ZnO	48
3.3	Synthesis of Pluronic F-127 coated ZnO NPs	50
3.4	Characterisation	50
3.4.1	X-Ray Diffraction (XRD)	51
3.4.2	Field Emission Scanning Electron Microscopy (FESEM) and Energy Dispersive X-ray Spectroscopy (EDS)	54
3.4.3	Transmission electron microscopy (TEM)	55
3.4.4	Electron spectroscopic imaging	56
3.4.5	Ultraviolet-Visible UV-VIS optical spectroscopy	57
3.4.6	Fourier Transforms Infrared (FT-IR) Spectroscopy	59
3.4.7	Zeta potential measurement	60
3.5	The cell line and cell culture	62

3.5.1	Chemicals and reagents	62
3.5.2	Equipment and apparatus	63
3.5.3	Cell lines and cells cryopreservation	64
3.5.4	Complete medium preparation	64
3.5.5	Recovery of frozen cell line	65
3.5.6	Subculture of cell lines	65
3.5.7	Cells counting	66
3.6	Determination of optimum cell number for MTT assay	67
3.7	The in-vitro cytotoxicity evaluation of ZnO samples towards the normal human endothelial EA.hy926 cell lines	68
3.7.1	MTT assay for ZnO samples cytotoxicity evaluation	68
3.8	The in vitro anticancer activity and Photodynamic Therapy (PDT) of ZnO samples towards bladder cancer cells	70
3.8.1	The phototoxicity of UV irradiation exposure time on the cell viability	70
3.8.2	MTT assay for Inhibitory concentration (IC ₅₀) determination during PDT and anticancer	71
3.9	Spheroids assay (3D tumour)	73
3.10	Determination of apoptotic morphological changes using Hoechst 33342 stain and Rhodamine 123 stain	75
3.11	Measurement of intracellular reactive oxygen species (ROS) production	75
3.12	Detection of Zn ²⁺ ion released	76
CHAPTER 4 RESULTS AND DISCUSSION		78
4.1	Introduction:	78
4.2	X-ray Crystallographic Analysis	78
4.3	UV-vis for ZnO NPs optical properties	80
4.4	Zeta potential Analysis	82
4.5	Stability of ZnO NPs	84
4.6	FTIR spectra analysis	86

4.7	Morphological studies and surface Elemental mapping analysis	88
4.8	Formation mechanism of Pluronic F-127 coated ZnO NPs	93
4.9	Determination of optimum cell number for MTT assay	94
4.10	Cytotoxic effects of ZnO NPs on the human endothelial EA.hy926 normal cells	96
4.11	ZnO NPs anticancer activity in the absence of UV irradiation	101
4.12	The phototoxicity effect of UV irradiation exposure time towards the RT4 cell viability	106
4.13	ZnO NPs photodynamic therapy towards bladder cancer RT4 cell line	107
4.14	The selectivity index of ZnO NPs	111
4.15	The photodynamic therapy impact on spheroid assay	116
4.16	ZnO NPs induce the cancer cell death via apoptosis pathway	118
4.16.1	Determination of nuclear condensation by Hoechst 33342 stain	118
4.16.2	Detection of mitochondrial membrane potential by Rhodamine 123 stain	120
4.17	Zinc ion release detection	122
4.18	ROS detection	124
4.19	The ZnO NPs cytotoxicity mechanism	127
CHAPTER 5 CONCLUSION AND FUTURE WORK		131
5.1	Conclusion	131
5.2	Future research direction	132
REFERENCES		133
LIST OF PUBLICATIONS		

LIST OF TABLES

		Page
Table 2.1	Typical properties of ZnO [28, 29].	8
Table 2.2	The common types of ROS with their electron structures. The “x” designates an unpaired electron [61].	15
Table 2.3	The anticancer effects of ZnO NPs on different human cancer cell lines.	30
Table 2.4	The application of ZnO in photodynamic therapy.	38
Table 2.5	The difference between apoptosis and necrosis [169, 170].	47
Table 3.1	Chemicals and reagents.	62
Table 3.2	Equipment and apparatus.	63
Table 4.1	The structural parameters of bare and Pluronic F-127 coated ZnO NPs.	80
Table 4.2	The IC ₅₀ and SI data of both ZnO NPs for cytotoxicity test on normal cells, dark anticancer, and photodynamic therapy.	114
Table 4.3	The percentage of Zn ²⁺ ion released from bare and coated ZnO NPs in the media after 24 h with pH values of 5 and 7.	124

LIST OF FIGURES

		Page
Figure 2.1	Hexagonal wurtzite crystal structure of ZnO. Zn ions are bonded to four O ions at the corners of a tetrahedron and vice versa [31].	9
Figure 2.2	The rock salt (left) and zinc-blende (right) structure models of ZnO [34].	10
Figure 2.3	PL spectrum (left) and UV-vis spectrum (upper right) of ZnO nanostructure at room temperature [38].	11
Figure 2.4	The main two cytotoxicity mechanisms of ZnO towards the normal cells.	14
Figure 2.5	The ROS levels and their impact on the cell [66].	16
Figure 2.6	The main key factors that can influence the cytotoxicity of ZnO NPs [70].	19
Figure 2.7	The molecular weight and the structural formula of PF-127 block copolymer.	21
Figure 2.8	Pluronic micelle as drug delivery system [88].	22
Figure 2.9	Bladder cancer in its first stage [117].	25
Figure 2.10	TEM images of (A) uncoated ZnO NPs and (B) silica coated ZnO NPs revealed the shape and morphology of the NPs [133].	29
Figure 2.11	Schematic illustration of (A) the basic mechanism of PDT and (B) the general procedure for PDT in a clinical setting [135].	31
Figure 2.12	Selected milestones of the historical development of PDT [135].	32
Figure 2.13	Schematic illustration of photo-physiochemical process in photodynamic therapy [142].	34
Figure 2.14	The mechanisms of reactive oxygen species (ROS) generation in ZnO NPs photodynamic therapy [1].	36
Figure 2.15	Schematic illustration of photodynamic cancer therapy by ZnO nanorods loaded with chemotherapeutic agent [153].	41
Figure 2.16	The cell death process in apoptosis and necrosis [167].	46

Figure 3.1	Schematic illustration for experimental design.	49
Figure 3.2	Schematic illustration for Pluronic F-127 coated ZnO NPs preparation.	50
Figure 3.3	Schematic diagram of the basic geometry of X-ray diffractometer.	51
Figure 3.4	PANalytical X'pert PRO MRD PW3040 X-ray diffractometer.	53
Figure 3.5	The schematic diagram and the image of Field emission scanning electron microscope FESEM system (FEI Nova NanoSEM 450).	54
Figure 3.6	(A) schematic diagram of transmission electron microscopy (TEM) system (B) TEM model (Libra 120-Carl Zeiss).	56
Figure 3.7	(A) schematic diagram for a typical UV-Vis spectrometer. (B) UV-Vis Cary 5000 spectrophotometer (Varian, Inc.).	58
Figure 3.8	Schematic diagram for the essential features of FTIR spectrometer.	59
Figure 3.9	Schematic illustration of the electrical double layer.	61
Figure 3.10	The Zetasizer Malvern instrument (Nano ZS model, ZEN 3600).	61
Figure 3.11	Hemocytometer chamber.	67
Figure 3.12	The 96 wells plate with the formed formazan.	70
Figure 3.13	The UV exposure during the PDT process.	72
Figure 3.14	The principles of multicellular tumour spheroids preparation by the hanging-drop method.	74
Figure 4.1	XRD patterns for bare and Pluronic F-127 coated ZnO NPs.	79
Figure 4.2	UV-vis absorption spectra of bare and coated ZnO NPs.	81
Figure 4.3	The optical absorption spectra of bare and coated ZnO NPs.	82
Figure 4.4	Zeta potential distribution of ZnO NPs (A) bare ZnO (B) Pluronic F-127 coated ZnO NPs.	83
Figure 4.5	Schematic illustration for electrostatic stabilisation and steric stabilisation.	84

Figure 4.6	Schematic illustration for the steric stabilisation as a result of the Pluronic coating layer.	84
Figure 4.7	Time-dependent UV–vis absorption spectra for 48 h. (A) bare ZnO NPs (B) coated ZnO NPs.	85
Figure 4.8	FTIR spectra for bare ZnO NPs and Pluronic F-127 coated ZnO NPs.	87
Figure 4.9	FESEM micrographs and EDS spectra with surface elements percentage (A) bare ZnO NPs (B) Pluronic F-127 coated ZnO NPs.	89
Figure 4.10	TEM micrographs for ZnO NPs (A) bare ZnO (B) Pluronic F-127 coated ZnO.	90
Figure 4.11	Histogram of coated ZnO particle size distribution.	91
Figure 4.12	ESI mapping with TEM micrographs for ZnO NPs (A) bare ZnO (B) Pluronic F-127 coated ZnO.	92
Figure 4.13	The optical density of the absorbance over cell density that were seeded into 96 well plate for 24h (A) normal EA.hy926 (B) bladder cancer RT4.	95
Figure 4.14	Cell viability of in-vitro cellular cytotoxicity after 48 h treatment with different concentration of bare and Pluronic F-127 coated ZnO NPs.	97
Figure 4.15	The comparative effects of ZnO NPs with different concentrations on in-vitro EA.hy296 cells in MTT assay (A) bare ZnO (B) Pluronic F-127 coated ZnO. The cells were photographed by fluorescence microscope using 10X magnifications.	98
Figure 4.16	Cell viability of in-vitro anticancer effect against RT4 cells after 48 h treatment with different concentration of bare and Pluronic F-127 coated ZnO NPs.	102
Figure 4.17	The IC ₅₀ of bare and Pluronic coated ZnO NPs anticancer effect.	102
Figure 4.18	The comparative effects of ZnO NPs with different concentrations on in-vitro anticancer activity against RT4 cells in MTT assay (A) bare ZnO (B) Pluronic F-127 coated ZnO. The cells were photographed by a fluorescence microscope using 10X magnifications.	105
Figure 4.19	The effect of UV irradiation time on the cell viability of the RT4 cells.	107

Figure 4.20	Cell viability of in-vitro PDT effect against RT4 cells after 48 h treatment with different concentration of bare and Pluronic F-127 coated ZnO NPs.	109
Figure 4.21	The IC ₅₀ of bare and Pluronic coated ZnO NPs PDT effect.	109
Figure 4.22	The comparative effects of ZnO NPs with different concentrations on in-vitro PDT activity against RT4 cells in MTT assay (A) bare ZnO (B) Pluronic F-127 coated ZnO. The cells were photographed by a fluorescence microscope using 10X magnifications.	110
Figure 4.23	Schematic illustration of a possible mechanism for ZnO NPs to act as a photosensitizer in RT4 photodynamic therapy [156].	111
Figure 4.24	The IC ₅₀ of bare and coated ZnO NPs on (A) cytotoxicity effect on EA.hy926 cells (B) dark anticancer effect on RT4 cells (C) PDT effect on RT4.	113
Figure 4.25	The ZnO NPs PDT efficiency on the 3D spheroid tumour of RT4 cells at 4x magnification.	117
Figure 4.26	The photomicrographs depict the images of RT4 cells with Hoechst 33342 stain taken at 6 and 18 h after the PDT with bare and coated ZnO NPs. The arrows indicate the clear signs of nuclear condensation and fragmentation. The cells were photographed by a fluorescence microscope using 20X magnifications	119
Figure 4.27	The photomicrographs depict the images of RT4 cells with Rhodamine 123 stain taken at 6 and 18 h after the PDT with bare and coated ZnO NPs. The cells were photographed by a fluorescence microscope using 20X magnifications	121
Figure 4.28	The standard curve of Zn ²⁺ concentrations.	122
Figure 4.29	The percentage of fluorescence of both ZnO NPs samples to induce the intercellular ROS in (A) normal EA.hy926 under the dark condition (B) cancer RT4 cells in the dark (C) cancer RT4 cells during PDT.	126
Figure 4.30	Schematic illustration for the ZnO NPs cytotoxicity effect during PDT. (a) ZnO NPs induce the generation of reactive oxygen species (ROS). ROS can damage the DNA and other organelles. (b) At lower pH, ZnO NPs will be dissolved and release Zn ⁺² that can cause protein activity disequilibrium, leading to cell death.	129
Figure 4.31	The mechanism of ROS generation under UV irradiation.	130

LIST OF SYMBOLS

a	Basal plane lattice constant
A	Absorbance
c	Uniaxial lattice constant
E_g	Band gap
$hkil$	Miller indices
θ	Bragg's angle
m_e	Electron mass
e	Electron
V	Volt
ml	Milliliter
I	Intensity of beam
α	Absorption coefficient
h	Planck's constant
E	Energy
c	Speed of light
λ	Wavelength
$\cdot\text{HO}$	Hydroxyl radical
H_2O_2	Hydrogen peroxide
$\cdot\text{O}_2^-$	Superoxide anion
OH^-	Hydroxyl ion
$^1\text{O}_2$	Singlet oxygen
$^\circ\text{C}$	Degree Celsius
eV	Electron volt
keV	Kilo electron volt
mA	Milliampere

β	Full wave at half maximum
d_{hkl}	Inter-plane distance
ε_c	Lattice strain
ν	Frequency

LIST OF ABBREVIATIONS

ZnO	Zinc oxide
NPs	Nanoparticles
UV	Ultraviolet
UVA	Ultraviolet-A
PDT	Photodynamic therapy
PS	Photosensitizer
ROS	Reactive oxygen species
WHO	World Health Organization
MNCR	Malaysian National Cancer Registry
TEM	Transmission electron microscope
EFTEM	Energy-filtering Transmission Electron Microscopy
ESI	Electron spectroscopy imaging
FESEM	Field emission scanning electron microscopy
EDS	Energy dispersive X-ray spectroscopy
FTIR	Fourier transform infrared spectroscopy
HR-XRD	High-resolution X-ray diffractometer
DMEM	Dulbecco's Modified Eagle Medium
FBS	Fetal Bovine Serum
P/S	Penicillin-Streptomycin
PBS	Phosphate Buffered Saline
DMSO	Dimethyl sulfoxide
MTT	(3-(4,5-Dimethylthiazol-2-yl)-2,5diphenyltetrazolium bromide)

ATCC	American Type Culture Collection
3D-MCTS	The 3D multicellular tumour spheroids
H2DCFDA	2-7- dichlorodihydrofluorescein diacetate
AAS	Atomic Absorption Spectrometer
IC ₅₀	Inhibitory concentration
A.C.	Anti-cancer
rpm	Revolutions per minute
ppm	Parts per million
SD	Standard deviation
Zn	Zinc
O	Oxygen
pH	Power of hydrogen (Potential of hydrogen ion)
PCD	Programmed cell death (apoptosis)
VB	Valence band
CB	Conduction band
DNA	Deoxyribonucleic acid
PEO	Polyethylene oxide
PPO	Polypropylene oxide
PF-127	Pluronic F-127
PEG	Polyethylene glycol
EPR	Enhanced permeability and retention
NRs	Nanorods
NC	Nanocomposites
PL	Photoluminescence
FDA	Food and Drug Administration

**KESITOTOKSIKAN NANOPARTIKEL ZINK OKSIDA BERSALUT
PLURONIC F-127 DAN TERAPI FOTODINAMIKNYA TERHADAP
TITISAN SEL KANSER PUNDI URINARI RT4 MANUSIA**

ABSTRAK

Kanser pundi urinari adalah ketumbuhan yang paling biasa dalam sistem urinari dan merupakan salah satu daripada sepuluh kanser paling biasa yang boleh menjejaskan seluruh badan. Terapi fotodinamik (PDT) diratakan amat berguna dalam rawatan kanser dengan kepilihan yang tinggi dan kesan sampingan yang minimum. Walau bagaimanapun, bahan fotopeka yang diluluskan secara klinikal mempunyai beberapa kelemahan dengan kepilihan tumour yang terhad dan boleh menjejaskan sel normal yang sihat. Nanopartikel zink oksida (ZnO NPs) telah menunjukkan keupayaan yang menggalakkan dalam pelbagai penggunaan bioperubatan termasuk terapi kanser. Dalam kajian ini, untuk pertama kalinya, keupayaan ZnO NPs tak salut dan bersalut Pluronic sebagai pefotopeka untuk terapi fotodinamik berkesan terhadap titisan sel RT4 kanser pundi urinari telah dikaji secara sistematik. Keputusan FESEM dan TEM menunjukkan bahawa ZnO NPs bersalut Pluronic F-127 mempunyai saiz purata 80 nm di mana julat ketebalan salutan Pluronic F-127 adalah 3 nm hingga 7 nm. Proses salutan Pluronic meningkatkan kestabilan ZnO NPs dengan ketara dan tidak mengubah struktur berhablur dan sifat optik yang dikehendaki. Kesitotoksikan ZnO NPs tak salut dan bersalut Pluronic F-127 ke atas titisan sel EA.hy926 endotelium manusia telah dinilai menggunakan asai MTT dan pengimejan mikroskopi. Keputusan ujian kesitotoksikan menunjukkan bahawa pengubahsuaian Pluronic F-127 meningkatkan bioserasi ZnO NPs terhadap sel biasa dengan ketara. Had kesitotoksikan bagi ZnO NPs tak salut dan bersalut Pluronic F-127 telah dimulakan selepas kepekatan

24 $\mu\text{g ml}^{-1}$ dan 48 $\mu\text{g ml}^{-1}$ masing-masing. Dalam pada itu, aktiviti antikanser dan terapi fotodinamik bagi ZnO NPs tak salut dan bersalut Pluronik terhadap titisan sel RT4 kanser pundi urinari telah diselidik secara sistematik. Keputusannya menunjukkan bahawa proses salutan menambah baik aktiviti antikanser dan terapi fotodinamik ZnO NPs secara relatif. IC_{50} bagi ZnO NPs yang tak salut dan bersalut semasa penyelidikan antikanser tanpa penyinaran UV adalah kira-kira 29.6 $\mu\text{g ml}^{-1}$ dan 27.4 $\mu\text{g ml}^{-1}$ masing-masing. Nilai ini berkurangan sehingga 22.9 $\mu\text{g ml}^{-1}$ untuk ZnO NPs yang tak salut dan 21.2 $\mu\text{g ml}^{-1}$ untuk ZnO NPs bersalut di bawah penyinaran UV semasa proses terapi fotodinamik. Tambahan pula, kesan terapi fotodinamik selepas 48 jam menggunakan kepekatan IC_{50} bagi ZnO tak salut dan bersalut ke atas tumour sferoid 3D bagi sel-sel RT4, menghalang agregasi tumour dengan kira-kira 35% dan 47% masing-masing bagi ZnO NPs yang tak salut dan bersalut. Keputusan ini merujuk kepada kestabilan yang tinggi dan kesebaran ZnO NPs bersalut yang bercas negatif dalam media akueus dibandingkan dengan ZnO NPs yang tak salut yang membenarkan lebih ZnO NPs bersalut saling tindak dengan sel-sel kanser, yang seterusnya menyebabkan pembebasan ion zink dan penjanaan spesies oksigen reaktif (ROS) di dalam sel-sel kanser, yang membawa kepada kematian melalui apoptosis.

**PLURONIC F-127 COATED ZINC OXIDE NANOPARTICLES
CYTOTOXICITY AND THEIR PHOTODYNAMIC THERAPY TOWARDS
HUMAN RT4 URINARY BLADDER CANCER CELL LINES**

ABSTRACT

Bladder cancer is the most common malignancy of the urinary system and one of the ten most common cancers that can affect the whole-body. Photodynamic therapy (PDT) holds promising applications in cancer treatment with high selectivity and minimum side effects. However, the current clinically approved photosensitizers have several drawbacks with limited tumour selectivity that affects the healthy normal cells. Zinc oxide nanoparticles (ZnO NPs) have exhibited promising potential in various biomedical applications including cancer therapy. In this study, for the first time, the potential of bare and Pluronic coated ZnO NPs as photosensitizers for effective photodynamic therapy against bladder cancer RT4 cell line were systematically investigated. The FESEM and TEM results revealed that Pluronic F-127 coated ZnO NPs had an average size of 80 nm whereby the Pluronic F-127 coating layer thickness ranged from 3 nm to 7 nm. The Pluronic coating process remarkably enhanced the stability of ZnO NPs and did not alter their desired crystalline structure and optical properties. The cytotoxicity of bare and Pluronic F-127 coated ZnO NPs on the human endothelial EA.hy926 cell line were evaluated through MTT assay and microscopy imaging. The results of the cytotoxicity tests showed that Pluronic F-127 modification significantly improved the biocompatibility of the ZnO NPs towards the normal cells. The cytotoxicity limit for bare and Pluronic F-127 coated ZnO NPs initiated after the concentration of 24 $\mu\text{g ml}^{-1}$ and 48 $\mu\text{g ml}^{-1}$ respectively. Furthermore, the anticancer activity and the photodynamic therapy of the bare and Pluronic coated ZnO NPs

against bladder cancer RT4 cell line were investigated. The results indicated that the coating process relatively improved the ZnO NPs anticancer activity and photodynamic therapy. The IC_{50} of bare and coated ZnO NPs during the anticancer investigation without UV irradiation was about $29.6 \mu\text{g ml}^{-1}$ and $27.4 \mu\text{g ml}^{-1}$ respectively. This value decreased to $22.9 \mu\text{g ml}^{-1}$ for bare ZnO NPs and $21.2 \mu\text{g ml}^{-1}$ for coated ZnO NPs under UV irradiation during the photodynamic therapy process. Moreover, the effect of photodynamic therapy after 48 h of using the IC_{50} concentration of bare and coated ZnO on the 3D spheroid tumour of RT4 cells, inhibits the tumour aggregation with about 35% and 47% for bare and coated ZnO NPs respectively. These outcomes referred to the high stability and dispersity of negatively charged coated ZnO NPs in the aqueous media as compared to bare ZnO NP that allowed for more coated ZnO NPs to be interact with cancer cells, which in turn induced the zinc ion released and the generation of reactive oxygen species (ROS) inside the cancer cells, leading to their death via apoptosis.

CHAPTER 1

INTRODUCTION

1.1 Nanotechnology

“There’s plenty of room at the bottom” - by this statement, the American physicist R. Feynman was the first to claim that the materials can be altered at the level of atoms and the idea of nanotechnology was initiated [1]. Nanotechnology is a scientific field that concern about synthesising, structuring, and the application of materials that have at least one dimension with a nanometric scale below than 100 nm [2]. These materials with their nano-dimension showed a unique physiochemical and biological properties that have been widely utilised in the science, engineering and medicine. Recently, the semiconductor nanomaterials including metal oxide nanoparticles (NPs) emerged as promising materials in the biomedical applications including cancer therapy, cell imaging, bio-sensing and drug delivery. One of these metal oxide nanoparticles that has been widely used in the biomedical application is zinc oxide (ZnO) NPs.

1.2 Zinc Oxide

ZnO NPs are inorganic semiconductor materials with wide direct band gap of about 3.37eV [3]. Moreover, ZnO is a low cost, non-toxic and biocompatible material that has been recognised as biosafe substance by the Food and Drug Administration (21CFR182.8991) [4]. In addition, ZnO is a biodegradable material that can be degraded to zinc ions which could be completely utilised in the biological systems as nutrients [5, 6]. Therefore, ZnO NPs are widely used in many applications, such as cosmetics, fillings in medical materials, antimicrobial materials, bio-imaging, and drug

delivery [7]. In addition, ZnO NPs have been considered as a promising treatment for cancer diseases [8].

1.3 Cancer

Cancer, which is also known as malignant tumours, is a group of diseases that characterised by uncontrolled cell proliferation of abnormal cells in the form of a tumour, that can invade the nearby tissue and spread to other body organs or tissue. If the spread is not controlled, it can result in death [9]. There are different types of cancer that are named based on the organs or the position where a malignant growth emanates such as bladder cancer.

1.4 Photodynamic therapy

Photodynamic therapy (PDT) is a novel promising clinically approved modality for effective cancer treatment [10, 11]. PDT consists of three essential nontoxic components: a photoactive agent such as ZnO or dye known as a photosensitizer (PS), harmless light with suitable wavelength, and molecular oxygen which presents in the biological cell. The PDT process involves the administration of PS to accumulate in the tumour tissue followed by localised light irradiation of a suitable wavelength that can activate the PS, leading to series of photochemical reactions to generate a highly cytotoxic reactive oxygen species (ROS) that kill the targeted cancer cells [12].

1.5 Motivation and Problem statement

Despite all the significant advances in the cancer therapy, cancer is still the second leading cause of death globally. According to the World Health Organization (WHO) estimation there were more than 18 million new cases that have been diagnosed with invasive cancer during 2018 and more than 9 million death cases from cancer worldwide [13]. Based on the latest health facts published by the Malaysian National Cancer Registry (MNCR) in 2016, there were more than 100 thousand new cancer cases in Malaysia during the period from 2007 to 2011.

Bladder cancer is a malignant tumour that originates from the epithelial lining of the urinary bladder. It is the most common malignancy of the urinary system and one of the ten most common cancers that can affect the whole-body [14, 15]. Moreover, bladder cancer has the highest recurrence rate (up to 80%) among any other known cancer and the metastasis and recurrence of advanced bladder cancer are the major causes of death [16]. Conventional therapy for bladder cancer involves surgery followed by chemotherapy and radiation therapy to eliminate residual malignant cells. However, Radiotherapy and chemotherapy have poor selectivity, that causes an elasticity loss to the irradiated area, reduction in platelets and red blood cells, mouth ulcers, hair loss, fatigue and reduction in the immune system of the patient [17-20]. Therefore, photodynamic therapy (PDT) that uses classic photosensitizers is introduced as promising new modality for the treatment of bladder cancer because it has a better selectivity for tumour with fewer side effects as compared to the radiation therapy and chemotherapy [21, 22]. However, the clinical application of PDT is severely restricted due to the shortcomings of the classic photosensitisers, including their low water solubility which makes them aggregate easily in the biological fluids, and more importantly, they exhibit limited tumour selectivity [23]. On the other hand,

ZnO NPs with their unique optical properties can generate reactive oxygen species (ROS) under UV irradiation, thus allowing them to behave as photosensitizers for PDT. However, the cytotoxicity of ZnO NPs towards different animal systems and cell lines have been reported [24, 25]. In addition, the aggregation of ZnO NPs and their poor solubility in the biological environment, resulting in low photo-reactivity which in turn reduce their activity in the cancer photodynamic therapy [26, 27]. Therefore, this thesis introducing Pluronic F-127 coated ZnO NPs as promising photosensitiser for RT4 bladder cancer PDT which expected to have a better stability and biocompatibility, with high tumour selectivity. Based on the literature review, there is no previous report regarding the use of Pluronic F-127 coated ZnO NPs as photosensitizers for RT4 bladder cancer photodynamic therapy.

1.6 Objectives

- 1- To investigate the structural, morphological and optical characteristics of Pluronic F-127 coated ZnO NPs.
- 2- To study the cytotoxicity impact of Pluronic F-127 coated ZnO NPs towards the endothelial AE.hy926 human normal cell line and RT4 bladder cancer cell line.
- 3- To investigate the efficiency of Pluronic F-127 coated ZnO NPs as photosensitizers for RT4 bladder cancer cell line photodynamic therapy.

1.7 Scope of the study

In this study, ZnO NPs have been coated with Pluronic F-127 and the impact of surface modification process on the structural, morphological, and optical properties of the ZnO NPs was investigated. In order to evaluate the cytotoxicity and the effect of modification on the biocompatibility of ZnO NPs, the human endothelial EA.hy926

cell line was used. Moreover, the anticancer impact of bare and PF-127 coated ZnO NPs towards RT4 bladder cancer cell line was investigated. In addition, the main scope of this study was to evaluate the bare and Pluronic F-127 ZnO NPs efficiency as photosensitizers for RT4 bladder cancer cell line photodynamic therapy.

1.8 Thesis Originality

The originality of this work can be summarised in these following points.

- The cytotoxicity study of Pluronic F-127 coated ZnO NPs on the EA.hy296 human endothelial cell line by using the MTT assay.
- The anticancer evaluation of Pluronic F-127 coated ZnO against RT4 bladder cancer cell line by using the MTT assay.
- The evaluation of bare and Pluronic F-127 coated ZnO NPs as photosensitizers for RT4 bladder cancer cell line photodynamic therapy.

1.9 Thesis outline

This thesis consists of five chapters and organised as follows: **Chapter 1** demonstrates a brief introduction to the current study, the motivation and problem statement, objective, scope and the originality of this thesis. **Chapter 2** presents the characteristics of ZnO NPs and their toxicity mechanisms as well as the properties of Pluronic F-127 material and its biomedical applications. Moreover, the general principles and a brief review on ZnO NPs anticancer activity and photodynamic therapy have been demonstrated. **Chapter 3** describes the ZnO NPs coating process as well as the methodology and the instrumentation used for the characterisation of bare and coated ZnO NPs. The cell culture, cytotoxicity and photodynamic therapy protocols are also briefly described in this chapter. **Chapter 4** presents the result and

the discussion of the synthesise of coated ZnO NPs as well as the characterisation results of bare and coated ZnO NPs. Moreover, it reports the results and the discussion of the cytotoxicity, anticancer and photodynamic therapy evaluation of bare and coated ZnO NPs. Finally, **Chapter 5** summarises the thesis findings and suggests future work.

CHAPTER 2

LITERATURE REVIEW

2.1 Introduction

The theories and the general principles of the subjects connected to this research are displayed in this chapter. Initially, the physical and optical properties of ZnO are addressed. Subsequently, the principles of ZnO NPs toxicity (mechanism and main key factors) are discussed. A general overview of Pluronic F-127 as a surfactant and its properties for biomedical application is presented. In addition, bladder cancer characteristics and its conventional treatments followed by an overview of ZnO NPs anticancer activity are introduced. The photodynamic therapy principles and a review of ZnO NPs as a photosensitizer in photodynamic therapy against cancer cell lines are also presented. Finally, an overview of the cell death morphological patterns are included.

2.2 Zinc Oxide

ZnO is an intrinsically n-type, metal oxide, semiconductor material that belongs to II-VI group with a direct wide band gap energy of 3.37eV and a large exciton binding energy of 60 meV at room temperature [3]. Moreover, ZnO is a cheap, non-toxic and biocompatible material that has been recognised as bio-safe substance by the Food and Drug Administration (21CFR182.8991) [4]. Moreover, ZnO is a biodegradable material that can be degraded to zinc ions which could be completely utilised in the biological systems as nutrients [5, 6]. Several properties of zinc oxide are summarised in Table 2.1.

Table 2.1 Typical properties of ZnO [28, 29].

Properties	Values
Lattice constants (T=300 K):	$a_o = b_o = 0.3247 \text{ nm}$
	$c_o = 0.5207 \text{ nm}$
Density	5.606 g/cm ³
Melting point	2248 K
Gap Energy	3.37 eV, direct
Exciton binding energy	60 meV
isoelectric point	9.5
(₃₀Zn) electron configuration	1S ² 2S ² 2P ⁶ 3S ² 3P ⁶ 3d ¹⁰ 4S ²
(₈O) electron configuration	1S ² 2S ² 2P ⁴
Molar mass	81.408 g/mol
Solubility in water	0.16 mg/100 mL
Stable crystal structure	Wurtzite
Refractive index	2.004
Electron mobility (T=300K)	200 cm/Vs
Hole mobility (T=300 K)	5-50 cm/Vs

2.3 ZnO crystal structure

The crystal structure of ZnO can be characterised as several alternating planes that consisting of tetrahedral zinc (Zn^{2+}) and oxygen (O^{2-}) ions that are located alternatively along c-axis. ZnO has three crystallisation forms: cubic zinc- blende, cubic rock-salt and hexagonal wurtzite structure. Under atmospheric pressure and

temperature, ZnO crystallises in the wurtzite hexagonal structure which is the most stable phase between the three crystallisation forms. Figure 2.1 illustrates the crystal model of the wurtzite hexagonal ZnO structure. This structure consists of alternating zinc (Zn^{2+}) and oxygen (O^{2-}) ions, where each zinc cation (Zn^{2+}) is bonded tetrahedrally by four oxygen anions (O^{2-}) and vice versa. The wurtzite lattice parameters $a = b = 0.3249$ nm laying in the x-y plane, including an angle of 120° , and $c = 0.5207$ nm which is parallel to the z-axis. [28, 30].

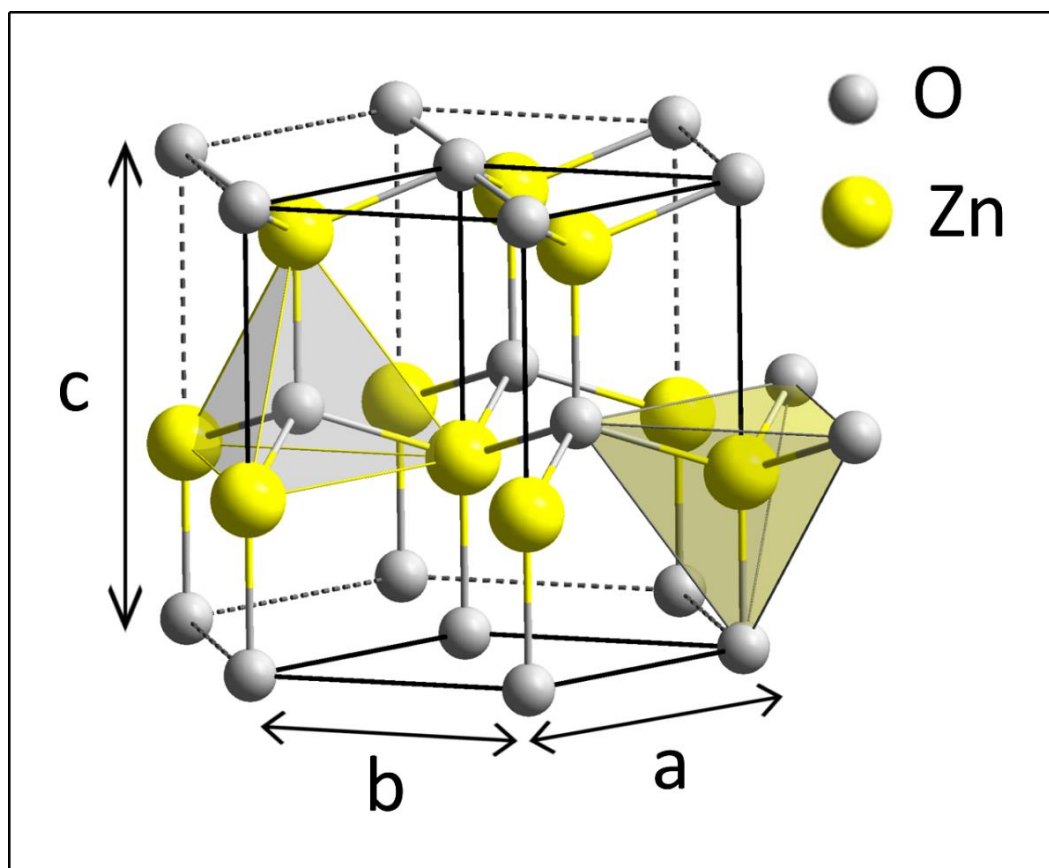


Figure 2.1 Hexagonal wurtzite crystal structure of ZnO. Zn ions are bonded to four O ions at the corners of a tetrahedron and vice versa [31].

Beside the hexagonal wurtzite structure for ZnO, the cubic zinc-blende and the rock salt structure models are demonstrated in Figure 2.2. The cubic zinc-blende ZnO structure can be stable only by the synthesis on cubic structure substrate like ZnS,

while the rock salt structure of ZnO can be obtained at relatively high pressure of about 100-kilobar [32, 33].

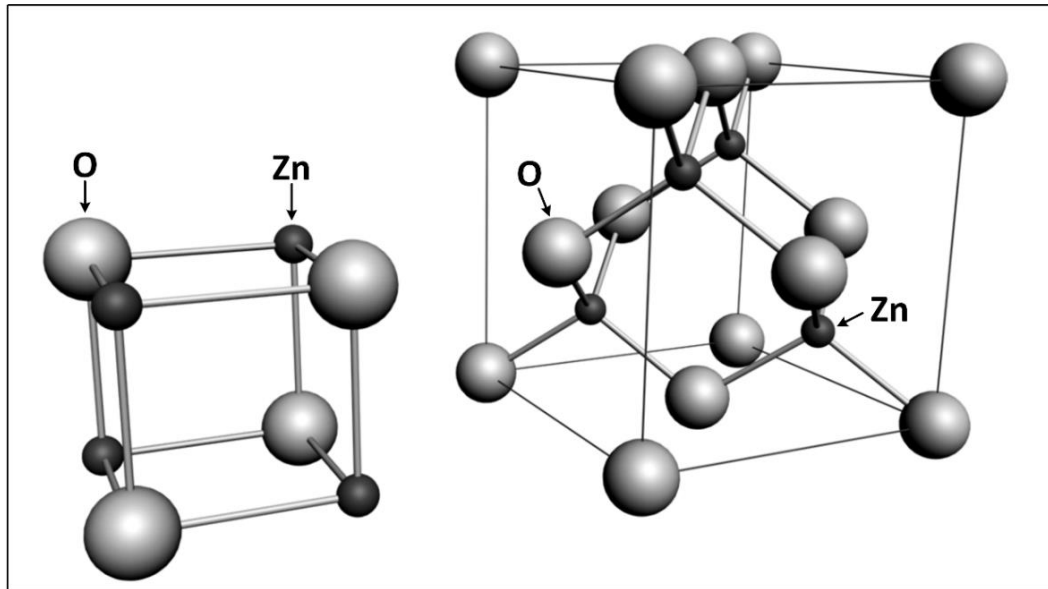


Figure 2.2 The rock salt (left) and zinc-blende (right) structure models of ZnO [34].

2.4 Optical properties

The ZnO optical properties have been widely studied through the photoluminescence (PL) and ultraviolet-visible (UV-Vis) spectra at room temperature [35]. In general, the ZnO PL spectrum consists of a near-band-edge emission (NBE) peak and a deep level emission (DLE) peak. The NBE peak is observed at UV wavelength region of approximately 380 nm (3.26 eV), which is attributed to exciton recombination. These intrinsic optical transitions take place between the electrons in the conduction band and holes in the valence band. The deep level emission (DLE) broad peak is observed near the green light wavelength, which is related to ZnO extrinsic optical properties that are associated with native defects emissions of ZnO [3, 36]. On the other hand, the UV-Vis spectrum demonstrates the measurement of the light beam attenuation that passes through the sample to give various spectrum of,

transmittance, absorbance and reflectance measurements in the UV, visible light and near-infrared wavelength range for both opaque and transparent ZnO samples. In general, the absorbance spectrum of the ZnO nanostructure shows high transparency in the visible region ($\lambda > 400$ nm) and high absorption for short wavelengths ($\lambda < 400$ nm) [3]. The absorption of UV light occurs due to the photo-excitation process. Where the photons are absorbed to excite electrons from the valence band (VB) to the conduction band (CB), results in electron-hole pair formation. These transitions provide information about the optical properties of ZnO such as absorption coefficient and energy bandgap [37]. Figure 2.3 shows PL spectrum and UV-vis spectrum of ZnO nanostructure at room temperature.

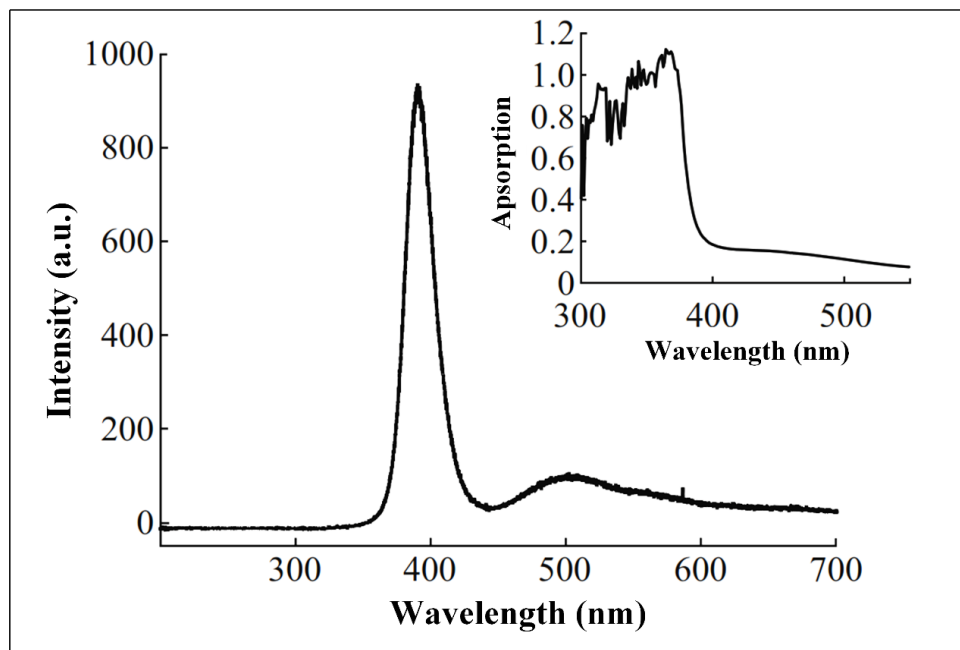


Figure 2.3 PL spectrum (left) and UV-vis spectrum (upper right) of ZnO nanostructure at room temperature [38].

However, the optical properties of the ZnO are strongly influenced by the energy bandgap structure [39, 40]. The fundamental absorption of radiation within the direct bandgap semiconductors such as ZnO occurs due to the photoexcitation of an

electron from the valence band (VB) to the conduction band (CB). Therefore, the direct energy bandgap can be determined by measuring the absorbed photon energy ($h\nu$) or the absorption coefficient (α) as a function of wavelength (λ). The intensity of the incident light after being transmitted through the semiconductor specimen can be given by [41]:

$$I_x = I_o e^{-\alpha x} \quad (2.1)$$

Where I_o is the incident light intensity, and I_x is transmitted light intensity after coming out of the specimen, and x is the specimen thickness. The absorbance (A) can be measured from the incident and transmitted light by Beer's law [42].

$$A = \log_{10} \left[\frac{I_o}{I_x} \right] \quad (2.2)$$

Therefore, the absorption coefficient can be calculated from the absorbance data using the following formula.

$$\alpha = \frac{2.303A}{x} \quad (2.3)$$

Where A is the absorbance, and x is the specimen thickness. The relation between the absorption coefficient (α) and the incident photon energy ($h\nu$) can be determined by using Tauc's relationship in the high absorption region of the spectrum [43].

$$(\alpha h\nu)^2 = C(h\nu - E_g) \quad (2.4)$$

Where E is the direct bandgap energy and C is a constant associated with the transition probability. Experimentally, the optical direct bandgap energy of ZnO sample can be calculated by the extrapolation of the linear portion of $(\alpha h\nu)^2$ versus $h\nu$ plots using Tauc's formula for the obtained data from the optical absorption spectra [43].

2.5 Toxicity of ZnO: Mechanism and main key factors

ZnO NPs with their unique structure and optical absorption properties are widely used in many biomedical applications such as cosmetics, fillings in medical materials, antimicrobial materials, bio-imaging, and drug delivery [7, 44]. Therefore, the biological safety of the ZnO NPs and their cytotoxicity impact have received a wide attention and became a hot research area by many researchers. Despite the widespread use of ZnO NPs, their toxicity towards different animal systems and cell lines have been reported. The results revealed that bare ZnO NPs were highly toxic towards different types of living cells and could cause a hazardous effect on the animal's body organs [45-47]. On the other hand, many research studies have reported that ZnO nanoparticles have shown selective toxicity towards cancer cells as compared with normal cells [7]. It has been reported that ZnO NPs exhibited 28-35 selective killing towards cancer cell as compared with normal cells [48]. Moreover, ZnO NPs have preferential cytotoxicity towards cervical cancer (HeLa) cell line as compared with normal (L929) cell line [49]. Despite of these toxicity studies, the hazardous effects of ZnO NPs are still debatable and unclear [24]. However, there are two main basic mechanisms behind the cytotoxicity of ZnO NPs as illustrated in Figure 2.4; the intercellular zinc ions (Zn^{2+}) releasing from the ZnO NPs, and the generation of reactive oxygen species (ROS) [50].

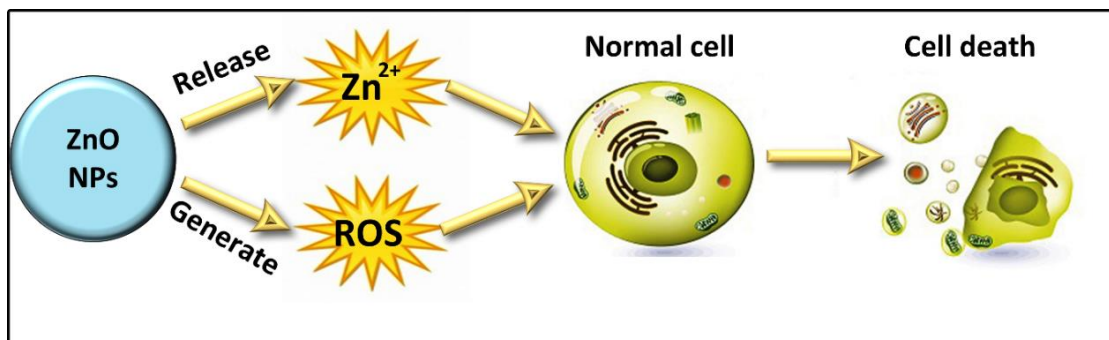


Figure 2.4 The main two cytotoxicity mechanisms of ZnO towards the normal cells.

2.5.1 The intercellular release of (Zn^{2+}) from the ZnO NPs

Zinc is one of the elements that is found with a certain concentration inside the human body cells [51]. Zinc plays an essential role in mammalian enzymes, gene expression, DNA damage repair, immune system and apoptosis regulations [52, 53]. Therefore, the changes in the zinc concentration can cause a severe problem in the cellular processes. However, the released Zn^{2+} from ZnO NPs was reported as the most toxic mechanism for ZnO NPs [54]. The intracellular release of zinc ions would increase the concentration of zinc ions from its normal level, resulting in zinc-mediated protein activity disequilibrium, which has a significant impact on the cellular processes, leading to cytotoxicity impact towards the cell [55, 56]. It has been reported that the Zn^{2+} dissolution rate increases as the pH decreases. Thus, the highly acidic microenvironment of cancer cells could induce the toxicity of ZnO NPs against the cancer cells while leaving the normal cell unaffected [57]. Indicating that the low pH is necessary for releasing the Zn^{2+} , thus the release of Zn^{2+} in extracellular fluid or blood that has a normal pH =7.4 is not preferable. However, the increment of Zn^{2+} can also increase the intercellular ROS which leads to cell cytotoxicity by oxidative stress [50, 58, 59].

2.5.2 The generation of reactive oxygen species (ROS)

Reactive oxygen species (ROS) or Oxygen-derived species are a collective term of radical and non-radical chemical species that contains oxygen, such as hydroxyl radical ($\cdot\text{OH}$), hydrogen peroxide (H_2O_2), superoxide anion ($\cdot\text{O}_2^-$), and hydroxyl ion (OH^-) [60]. Table 2.2 illustrates the common types of ROS with their electron structures.

Table 2.2 The common types of ROS with their electron structures. The “x” designates an unpaired electron [61].

Electron structures of ROS	$\times \ddot{\text{O}}::\ddot{\text{O}}:$	$\times \ddot{\text{O}}::\ddot{\text{O}}\times$	$\text{H}:\ddot{\text{O}}::\ddot{\text{O}}:\text{H}$	$\times \ddot{\text{O}}:\text{H}$	$:\ddot{\text{O}}:\text{H}$
ROS	Superoxide anion ($\cdot\text{O}_2^-$)	Peroxide ($\cdot\text{O}_2^-$)	Hydrogen peroxide (H_2O_2)	Hydroxyl radical ($\cdot\text{OH}$)	Hydroxyl ion (OH^-)

However, (ROS) are produced inside the cell with certain physiological concentrations during various cellular processes such as inflammatory response, mitochondrial respiration, microsomes activity and play an essential role in cell signalling and homeostasis [62]. At medium levels of ROS generation, the cells will induce the cellular antioxidant defensive response to proceed their survival. In contrast, at high levels of ROS, the disequilibrium between the ROS formation and the efficiency of antioxidative systems initiate oxidative stress that possesses a serious danger to the integrity of cells and their correct functioning, leading to cellular damage [63-65]. Figure 2.5 illustrates the ROS levels and their impact on the cell.

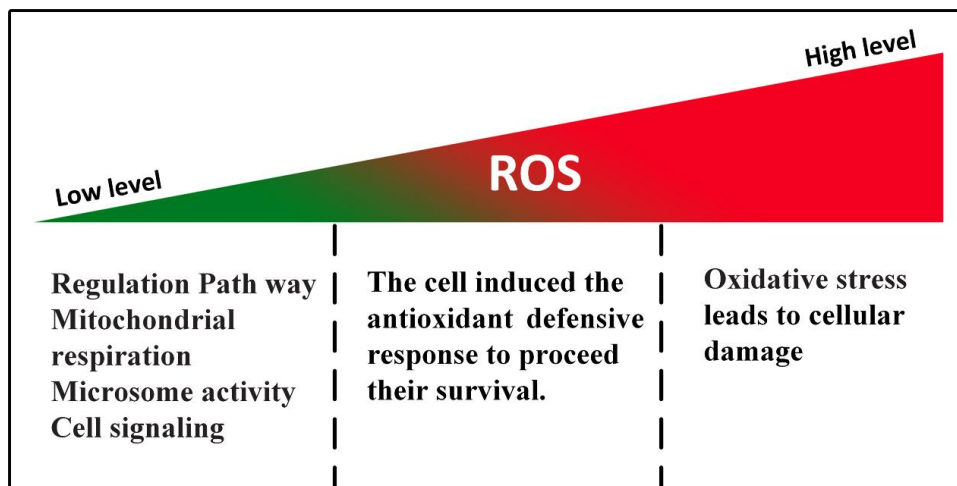
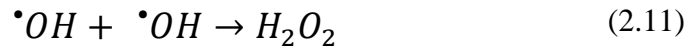
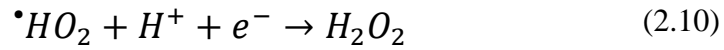
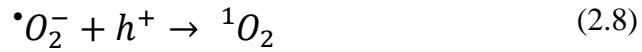
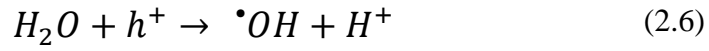
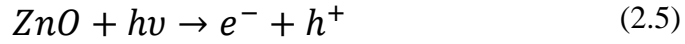


Figure 2.5 The ROS levels and their impact on the cell [66].

However, metal oxide NPs including ZnO NPs induce the ROS production as one of their basic mechanisms for intercellular toxicity. The ZnO NPs induce the intercellular ROS by the cells' inflammatory response against the NPs and by the redox reactions that occurs at the ZnO NPs surface [67]. ZnO NPs can generate the intercellular ROS under the UV light and in the dark conditions [68].

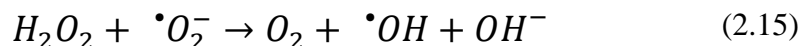
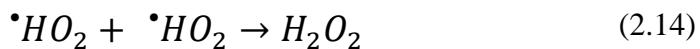
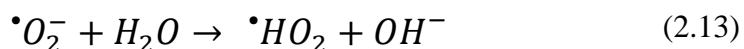
2.5.2.(a) Mechanism of ROS generation under UV light

The generation of ROS by ZnO NPs under UV light is well reported. The ability of ZnO NPs to produce ROS under UV irradiation is due to their semiconductor properties with a wide direct band gap of 3.37 eV. Thus, by using photon energy such as UV light, the electrons (e-) from the valence band will be excited to reach the conductive band and leaving behind holes (h+) at the valence band. These electrons (e-) and holes (h+) can interact with cellular molecules (O₂, H₂O) within the cellular aqueous microenvironment and generate the ROS formations. Furthermore, radiative recombination of the electron-hole pair can generate emission of photon that can excite the oxygen ground state to generate singlet oxygen (¹O₂). All these ROS, can cause a highly cytotoxic impact and thus, promoting the cell death [67]. The ROS generation in light is given by these equations [69].



2.5.2.(b) Mechanism of ROS generation in dark

Lakshmi and Vijayaraghavan have proposed the mechanism of ROS production in the dark. Where oxygen from the ambient environment can react with electrons from the surface of ZnO NPs to form a superoxide radical ($\cdot\text{O}_2^{-}$) as reported in a sensor study. Then, the superoxide within the aqueous environment can solvate to form hydroperoxyl radicals. The hydroperoxyl radicals ($\cdot\text{HO}_2$) can recombine to form hydrogen peroxide H_2O_2 . Subsequently, the hydrogen peroxide may react with superoxide radical to form hydroxyl radical and hydroxyl ion. However, in the dark mechanism, singlet oxygen (${}^1\text{O}_2$) generation is not possible, as a hole is required for its generation which will not be produced. The ROS generation in dark is given by these equations [69].



However, The mechanism for ROS generation is vary for each nanoparticles and to date the exact intercellular mechanism for ROS production is incompletely understood and needs more investigations [62].

2.5.3 Main toxicity key factors

The main key factors that result in toxicity of ZnO NPs towards the cell lines include particle size, surface properties and dissolution [70, 71]. A high surface area to volume ratio of nanoparticles allows a greater number of constituting atoms to be located around the surface of the NPs. Therefore, the size reduction to the nanoscale may result in a unique physiochemical and electrical properties that influence the toxicity of the NPs which are not present in the bulks [72]. Many studies have reported that nanosized particles always have more toxicity impact than bulks materials [70]. It has been reported that ZnO nanosized particles showed more cytotoxicity impact on (THP-1) cell line as compared with its micro-sized particles [73]. Moreover, the cytotoxicity of different sized ZnO NPs (20, 60, 100 nm) towards SMMC-7721 cancer cells has been demonstrated. The study revealed the size-dependent effect was not clear within the size range from 20 nm to 100 nm [74]. In addition, some studies have revealed that NPs with a size range from 10 - 100 nm, can hardly be up-taken by

healthy cells while they can easily penetrate tumour cells [75]. Figure 2.6 Illustrates the main key factors that can influence the cytotoxicity of ZnO NPs.


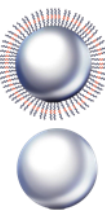

Size		<p>ZnO NPs always showed more serious toxicity than bulks.</p>
Surface		<p>Surface charge plays a critical role in the NPs cytotoxicity profile. Positively charged NPs could be more toxic towards healthy normal cells as compared with cancer cells. Positively charged nanoparticles could penetrate into the cells more easily.</p>
Dissolution		<p>ZnO NPs can be dissolved within the aqueous solution to form Zn²⁺ cations which considered to be one of the basics toxicity mechanisms for ZnO NPs.</p>

Figure 2.6 The main key factors that can influence the cytotoxicity of ZnO NPs [70].

Besides the size effect, researchers reported that surface characteristics such as surface charge plays a critical role in the nanoparticles' cytotoxicity profile [76-78]. Previous studies reported that NPs with a positive charge could be more toxic towards healthy normal cell lines, while nanoparticles with a negative charge internalise mostly in the cancer cell lines [78, 79]. It was also reported that the positively charged nanoparticles could penetrate into the normal cells more easily due to the electronic potential of the cell membrane that is known to be negative [76, 77, 80]. However, the surface physiochemical properties of the NPs can be adjusted by surface modification and functionalization. The surface functionalization of NPs can alter their surface charge, functionality, and reactivity with the cell lines. Moreover, it can improve the stability and dispersive ability of the core nanoparticles [81]. It has been reported that ZnO NPs surface modification with different capping agents (PEG and starch) was

found to influence the cytotoxicity of ZnO NPs towards the human osteoblast cancer cell line (MG-63), and the cytotoxicity of ZnO NPs was reduced by starch surface modification [82].

Another main key factor of cytotoxicity of ZnO NPs is their dissolution in the aqueous environment. ZnO NPs can be dissolved within the aqueous solution to form Zn^{2+} cations which considered to be one of the basics toxicity mechanisms for ZnO NPs. Under the acidic conditions, the dissolution of ZnO NPs increases. Thus, the Zn^{2+} cations increase. It has been reported that the cytotoxicity of ZnO NPs towards the phagocytic (RAW 264.7) and the human bronchial epithelial (BEAS-2B) cell lines was directly proportional to NPs dissolution, where the leaching of zinc ions disrupts the intercellular zinc homeostasis that in order leads to the cell death [83]. Recently, Chia et al. reported the use of silica as a surface modifier to reduce the toxicity of ZnO NPs. The results showed that the silica remarkably reduced the cytotoxicity of ZnO NPs towards Human colon cancer cell (SW480), and human colorectal adenocarcinoma epithelial cell (DLD-1) by preventing the dissolution of ZnO NPs to Zn^{2+} in aqueous solution [84]. It has been reported that the surface modification for ZnO quantum dots by amino-silane prevents ZnO QDs from dissolution and releasing Zn^{2+} cations. As a result, increased the biocompatibility of ZnO NPs [85]. In general, the surface modification of the ZnO NPs can improve their biocompatibility, stability and overcome the problem of ZnO NPs agglomeration [86].

2.6 Pluronic F127 surfactant

Recently, block copolymers have emerged as a potential coating or stabilising agent for targeted drug delivery, diagnostic imaging and gene therapy [87, 88]. One such promising block copolymers proposed for biomedical applications are Pluronic

(also known as poloxamers), that consist of a triblock PEO-PPO-PEO structure (PEO: polyethylene oxide, PPO: polypropylene oxide). Among these Pluronics, Pluronic F-127 (PF-127) is a commercially available biocompatible, nontoxic, injectable and thermo-reversible triblock copolymer that has been approved by the Food and Drug Administration (FDA) for humans [89, 90]. Pluronic F-127 is amphiphilic in nature with an average molar mass of 12600 that composed of a hydrophobic central segment of poly(propylene oxide) (PPO) flanked by two hydrophilic segments of poly(ethylene oxide) (PEO). The molecular weight and the structural formula of PF-127 block copolymer is shown in Figure 2.7.

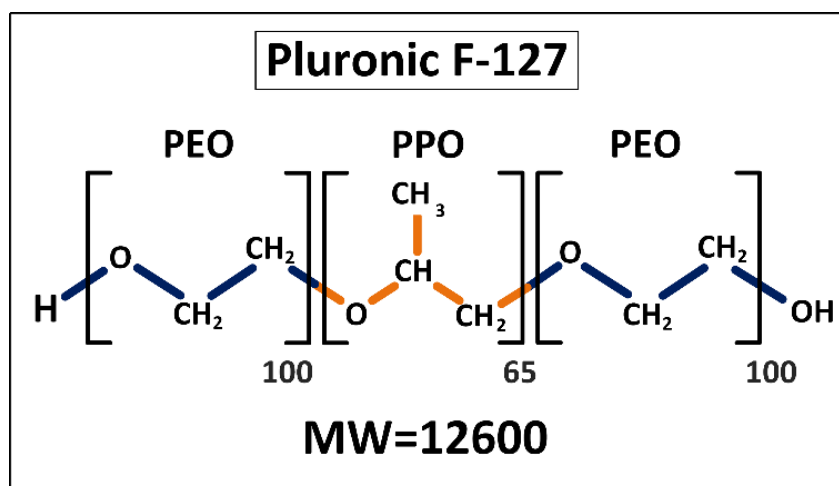


Figure 2.7 The molecular weight and the structural formula of PF-127 block copolymer.

However, PF-127 has been widely used as a coating or stabilising agent for nanoparticles surface modification in various biomedical applications [91, 92]. Moreover, Pluronic F-127 was found to be the least toxic and the most efficient polymer for colloidal stabilisation among many triblock copolymers in previous studies [93-96]. Furthermore, PF-17 showed an important biological role in drug delivery. It has been discovered that the PF-127 delivery system plays a role in

sensitising the multidrug-resistant cancer cells to the anti-cancer agents. Therefore increasing the efficacy of tumour thereby [97].

2.6.1 Pluronic F-127 as a surfactant for NPs in biomedical application

The unique thermo-reversible micellization characteristic of Pluronic F-127 around body temperature makes it desirable for drug delivery, controlled release, gene therapy and tissue engineering [98, 99]. Pluronic F-127 can be transformed from a low viscosity solution to semi-solid gel by heating. Therefore, when Pluronic F-127 is injected into body, the solution will form a semi-solid shell as a sustain release depot [96]. The high biocompatibility and the thermo-reversible characteristics have allowed PF-127 to be used as a promising drug delivery system for different routes of administration including topical, oral, intranasal, ocular, vaginal, rectal and parenteral routes [96, 100, 101].

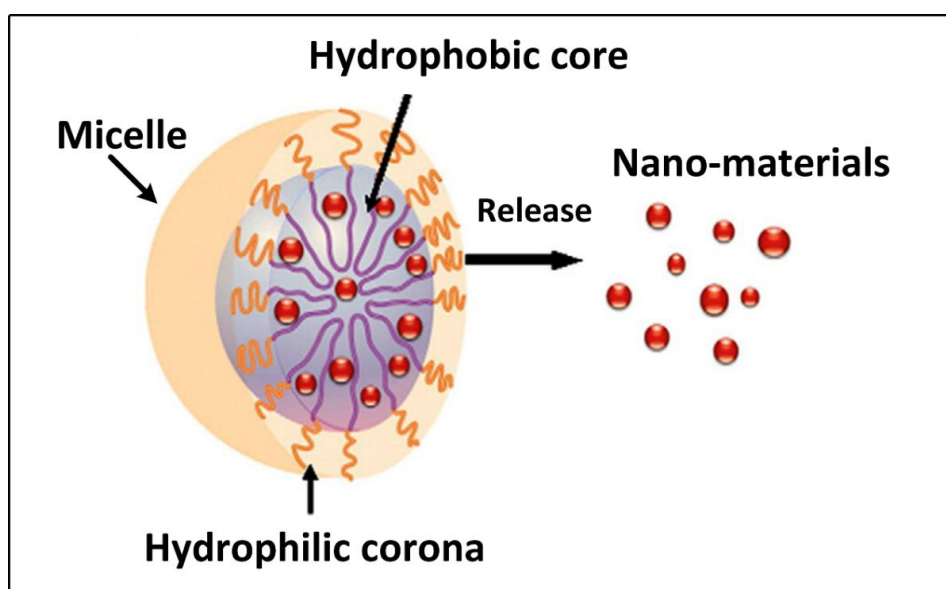


Figure 2.8 Pluronic micelle as drug delivery system [88].

Besides, an important application for Pluronic F-127 micelles is to carry the nano-materials in the core of the micelles (Figure 2.8). Pluronic F-127 micelles were

frequently used as a host to many nanoparticles to stabilise the dispersion of these particles in the aqueous solutions and improve their biocompatibility. Recently, Pluronic F-127 was utilised to synthesise thermo-responsive gels with gold nanoparticles for antibacterial and wound healing [102]. Pluronic F-127 micelles were used to encapsulate gold nanorods (NRs) to enhance their stability and biocompatibility in aqueous solution, the encapsulated gold nanorods were used as a biocompatible optical probe with capability for in vitro imaging [103]. Recent studies have shown that Pluronic F-127 micelles can also increase the stability and reduce the toxicity of gold nanoparticles for different biomedical applications [93, 104-106]. In addition, recent studies reported the use of Pluronic F-127 as a surfactant for silver nanoparticles in antibacterial applications [107-109]. Moreover, Pluronic F-127 was used to functionalize magnetite/graphene nanohybrid for chemo-phototherapy. Whereas, Pluronic F-127 improved the nanohybrid solubility and stability in a physiological environment [92]. Furthermore, researchers have reported that Pluronic F-127 improved the stability and the biocompatibility of magnetic nanoparticles for magnetic resonance imaging (MRI) and hyperthermia treatment [110, 111]. Moreover, quantum dots were encapsulated by Pluronic F-127 micelles to enhance the optical and colloidal stability of quantum dots in biological systems for in vivo cancer imaging [112].

2.6.2 Pluronic F-127 coated ZnO nanoparticles

Pluronic F127 was used as a crystal growth modifier to synthesise ZnO microspheres [113]. In addition, Pluronic F-127 was also used to control the growth shape of micro and nano-sized ZnO with different shapes [114]. Finally, Li et al. successfully fabricated a ZnO porous nanosheets after thermal treatment to zinc acetate nanosheets that had been synthesised by using the PF-127 as templets [115].

2.7 Bladder Cancer

Cancer, which is also known as malignant tumours, is a genetic disease that characterised by uncontrolled cell proliferation of abnormal cells in the form of a tumour, that can invade the nearby tissue and spread to other body organs or tissue (metastasis). If the spread is not controlled, it can result in death [9]. Cancer is a major health problem worldwide and is the second leading cause of death globally. According to the World Health Organization (WHO) estimation during 2018, there were 18,078,957 new cases that have been diagnosed with invasive cancer and about 9,555,027 death cases from cancer worldwide [13]. In the United States, there were around 1,7 million estimated new cases and over 609,640 American deaths from cancer in the same year [116]. Based on the latest health facts published by the Malaysian National Cancer Registry (NCR) in 2016, there were 103,507 new cancer cases in Malaysia during the period from 2007 to 2011. However, various types of cancers are named according to the organs or the sites where a malignant growth emanates.